Study on Initial Alignment Under Large Misalignment Angle

Qi Wang[1, 2, *], Changsong Yang[2, 4] and Shaoen Wu[3]

Abstract: Misalignment angle error model describing the SINS mathematical platform error is presented in this paper following the idea of small misalignment angle error model and large azimuth misalignment angle error model. It can be considered that the three misalignment angles are independent of the rotational sequence in the misalignment error model, but not suitable in the large misalignment error model. The error angle of Euler platform is used to represent the three misalignment angles from theoretical navigation coordinate system to computational navigation coordinate system. The Euler platform error angle is utilized to represent the mathematical platform error and its physical meaning is very clear. The SINS nonlinear error model is deduced by using the error angle of Euler platform and is simplified under the condition of large azimuth error and small error. The simplified results are more comprehensive and accurate than the large azimuth misalignment error model. The damping SINS algorithm and its error model are proposed to change the structure of the strapdown inertial navigation algorithm by using the external damping information. The accuracy of SINS error model of large Euler platform error angle is simulated, and has strong practicability in initial alignment and is conducive to reducing the amount of calculation.

Keywords: Misalignment error model, large misalignment angle, Euler platform error angle, SINS.

1 Introduction

Error propagation model and filtering algorithm are two important problems in the initial alignment of Strapdown Inertial Navigation System [Li, He, Zhang et al. (2017); Wei, Wang, Bai et al. (2017)]. The error sources of SINS usually include measurement errors of inertial devices, initial condition errors, environmental model errors (or earth model errors) and numerical algorithm errors [Metzger and Jircitano (1975); Qian, Liu and Li 2011)]. SINS error model is the basis of studying the error propagation characteristics of SINS and information fusion between multiple navigation systems [Zhang, Chen, Shi et

[1] School of Computer and Software, Nanjing University of Information Science and Technology, Nanjing, 210044, China.

[2] Jiangsu Engineering Center of Network Monitoring, Nanjing University of Information Science and Technology, Nanjing, 210044, China.

[3] Department of Computer Science, Ball State University, Muncie, USA.

[4] School of Automation, Nanjing University of Information Science and Technology, Nanjing, 210044, China.

[*] Corresponding Author: Qi Wang. Email: wangqi@nuist.edu.cn.

al. (2015)]. It plays an important role in initial alignment and integrated navigation applications [Sun, Wang and Gao (2009)]. The mathematical equations describing the SINS algorithm are a set of nonlinear differential equations. In the classical SINS error model with small misalignment angle [Xiong and Shi (2018)]. Based on a small perturbation to SINS equation caused by error factors by ϕ angle method or ψ angle method, a set of error models of linear differential equations are derived [Zhou, Li and Yang (2008)]. The linear error model of SINS with small misalignment angle is established only under the assumption that all kinds of error sources are small [Wang and Zhang (2011); Bishop (2002)]. With the development of SINS technology, initial alignment with large misalignment angle is the most representative, and the development of nonlinear filtering estimation technology [Fang, Zhang, Sheng et al. (2018)]. Error models are no longer confined to linear models [Feng, Shen and Chang (2003); Wu, Hou and Wang (2009)]. Some new error models are emerging, such as large azimuth error model, quaternion-based error model and dual quaternion-based error model [Fu, Wu, Wang et al. (2017); Xiong and Shi (2018); Zhao, Wu, Zhang et al. (2018)]. The misalignment error model of large azimuth is nonlinear. It requires that the level misalignment angle is small [Shu (2016); Yan, Xu, Zhang et al. (2013)). The error equation representing attitude in quaternion-based error model can be linear, but the physical meaning of each component of error quaternion is not clear. It also increases the dimension of error model, and the error equation representing velocity error is still nonlinear. The error model based on dual quaternion also has the problem of increasing dimension, which will inevitably increase the amount of filtering calculation. There is no literature about the application of this error model.

Extended Kalman Filter (EKF) is the most widely used in nonlinear filter [Meng, Rice, Wang et al. (2010)]. The basic principle of EKF is to linearize the nonlinear function, i.e., to ignore the influence of the higher order terms of Taylor expansion [Qu, Li, Xie et al. (2013); Liu and Liu (2010)]. When using EKF, we must know the exact expansion of the nonlinear function, and some improved algorithms, such as higher order truncated EKF and iterative EKF, are also derived from EKF [Salan, Eduardo and Hugh (1999); Huge, Steven and Louis (2004)]. The starting point of EKF filter is approximate nonlinear function, but the probability density distribution of general approximate nonlinear function is easier than approximate nonlinear function [Wu and Zhang (2003); Zhang, Xu, Liu et al. (2012)]. Nowadays, filter estimation methods based on approximate probability density distribution are popular, such as particle filter [PF)], which can evolve probability density distribution directly by solving nonlinear function through particle [sample point)] instead of knowing the specific expansion of nonlinear function in detail [Xu, Dong, Tong et al. (2017)); He and Cai (2006)].

2 Simplification and accuracy simulation of SINS error model

Obviously, it is complicated to expand the nonlinear error model of SINS according to each component, especially for the attitude error equation, but it can be simplified under some conditions to meet the specific application situation [Qu, Zhu, Wang et al. (2018); Xu, Yan, Ning et al. (2007)]. In the following analysis, it is assumed that the gyro

measurement error $\delta\omega_{ib}^{b}$ is mainly drift error ε^{b}, the accelerometer measurement error δf_{sf}^{b} is mainly bias error ∇^{b}, and the gravity error term δg^{n} is neglected, record as $\varepsilon^{n'}=\mathbf{C}_{b}^{n'}\varepsilon^{b}$, $\nabla^{n'}=\mathbf{C}_{b}^{n'}\nabla^{b}$ and $\widetilde{f}_{sf}^{n'}=\mathbf{C}_{b}^{n'}\widetilde{f}_{sf}^{b}$

2.1 SINS error model under large azimuth misalignment angle

Under the condition of large azimuth misalignment, it is assumed that α_x and α_y of Euler platform error angle are small, while α_z is arbitrary value. Then there is an approximation, $s\alpha_x\approx\alpha_x$, $c\alpha_x\approx 1$, $s\alpha_y\approx\alpha_y$, $c\alpha_y\approx 1$ and

$$\mathbf{C}_{\omega}^{-1}\approx\begin{bmatrix}1 & 0 & \alpha_y\\ 0 & 1 & \alpha_y\\ -\alpha_y & 0 & 1\end{bmatrix},\quad \mathbf{C}_{n}^{n'}\approx\begin{bmatrix}\mathrm{c}\alpha_z & \mathrm{s}\alpha_z & -\alpha_y\\ -\mathrm{c}\alpha_z & \mathrm{c}\alpha_z & \alpha_x\\ \alpha_y\mathrm{c}\alpha_z+\alpha_x s\alpha_z & \alpha_y s\alpha_z-\alpha_x c\alpha_z & 1\end{bmatrix} \tag{1}$$

By substituting these approximations into formulas (1), the higher order terms about other errors are omitted except azimuth errors.

$$\alpha=\mathbf{C}_{A}\widetilde{\omega}_{in}^{n}+\mathbf{C}_{\alpha_z}\delta\omega_{in}^{n}-\varepsilon^{n'} \tag{2}$$

$$\delta v^{n}=\mathbf{C}_{B}\widetilde{f}_{sf}^{n'}+\mathbf{C}_{\alpha_z}^{T}\nabla^{n'}-(2\delta\omega_{ie}^{n}+\delta\omega_{en}^{n})\times\widetilde{v}^{n}-(2\widetilde{\omega}_{ie}^{n}+\widetilde{\omega}_{en}^{n})\times\delta v^{n} \tag{3}$$

Among them

$$\mathbf{C}_{A}=\mathbf{C}_{\omega}^{-1}(I-\mathbf{C}_{n}^{n'})\approx\begin{bmatrix}1-c\alpha_z & -s\alpha_z & \alpha_y\\ s\alpha_z & 1-c\alpha_z & -\alpha_x\\ -\alpha_x s\alpha_z-\alpha_y & \alpha_x c\alpha_z & 0\end{bmatrix}$$

$$\mathbf{C}_{B}=I-(\mathbf{C}_{n}^{n'})^{T}\approx\begin{bmatrix}1-c\alpha_z & -s\alpha_z & \alpha_y\\ \mathrm{s}\alpha_z & 1-c\alpha_z & -\alpha_x\\ \alpha_y & -\alpha_x & 0\end{bmatrix}$$

In (2), there is an error distribution matrix $\mathbf{C}_{\alpha_z}$ before $\delta\omega_{in}^{n}$, and because α_z is not a small quantity, $\mathbf{C}_{\alpha_z}$ cannot be approximated as a unit matrix.

2.2 SINS error equation under small misalignment angle

Under the condition of small misalignment angle, the error angles of the three Eulerian platforms are small. Approximate $\mathbf{C}_{A}\approx(a\times)$, $\mathbf{C}_{B}\approx-(a\times)$, $\mathbf{C}_{\alpha_z}\approx I$ So (1) and (2) are further approximated to

$$\alpha=-\widetilde{\omega}_{in}^{n}\times a+\delta\omega_{in}^{n}-\varepsilon^{n'} \tag{4}$$

$$\delta v^n = \widetilde{f}_{sf}^{n'} \times a + \nabla^{n'} - (2\delta\omega_{ie}^n + \delta\omega_{en}^n) \times \tilde{v}^n - (2\widetilde{\omega}_{ie}^n + \widetilde{\omega}_{en}^n) \times \delta v^n \tag{5}$$

2.3 Damping SINS algorithm and its error model

The previous analysis is a complete strapdown inertial navigation algorithm and its error model. If the structure of the algorithm is changed, such as introducing external damping information into the algorithm, a more concise error model can be obtained. It is called damping SINS algorithm and damping SINS error model temporarily. The damping SINS algorithm and its error model are in the initial pair. It has important practical value. For example, in the initial alignment of SINS and GPS combined moving base, GPS can provide more accurate velocity v_g^n and position L_g, λ_g, h_g information. Or in the initial alignment of SINS quasi-stationary base (wireless or linear motion is very small but can have angular motion), the reference speed is zero and the geographical position is accurately known. In both cases, the reference speed or position information can be introduced into SINS algorithm. The SINS error model is simplified with GPS damping as an example, and the quasi-static base is similar. The basic method to establish the GPS damping SINS algorithm is to obtain the calculation parameters related to velocity and position from the known GPS information at the right end of Formula (1), that is, to rewrite Formula (1) to

$$\mathbf{C}_b^{n'} = \mathbf{C}_b^{n'}(\widetilde{\omega}_{nb}^b \times) \tag{6}$$

$$\tilde{v}^n = \mathbf{C}_b^{n'} \widetilde{f}_{sf}^b - (2\omega_{ie,g}^n + \omega_{en,g}^n) \times v_g^n + g_g^n \tag{7}$$

$$\tilde{L} = \frac{\tilde{v}_N^n}{R_{M,\mathrm{g}} + h_g}, \tilde{\lambda} = \frac{\tilde{v}_E^n \sec L_g}{R_{N,g} + h_g}, \tilde{h} = \tilde{v}_U^n \tag{8}$$

Among them $\widetilde{\omega}_{nb}^b = \widetilde{\omega}_{ib}^b - \mathbf{C}_{n'}^b \omega_{in,g}^n$ The term g in the subscript indicates that the GPS information is calculated by GPS information. If the GPS information error is small enough to be ignored and the relevant calculation parameters are equivalent to the real value, or no error, it is similar to the method of deriving the error model of SINS algorithm or the error model of SINS algorithm. Based on the proper simplification, the error model corresponding to the damped SINS algorithm (8) can be obtained.

$$a = \mathbf{C}_\omega^{-1}[(I - \mathbf{C}_n^{n'})\omega_{in,g}^n - \varepsilon^{n'}] \tag{9}$$

$$\delta v^n = [I - (\mathbf{C}_n^{n'})^T]\widetilde{f}_{sf}^{n'} + (\mathbf{C}_n^{n'})^T \nabla^{n'} \tag{10}$$

$$\delta L = \frac{1}{R_{M,\mathrm{g}} + h_g} \delta v_N^n, \delta\lambda = \frac{\sec L_g}{R_{M,\mathrm{g}} + h_g} \delta v_E^n, \delta h = \delta v_U^n \tag{11}$$

It can be seen that the differential equation of Euler platform error angle α does not contain the information of velocity error and position error, and the differential equation of velocity error δv^n does not contain the information of position error. Initial alignment

of Euler platform error angle information using damped SINS algorithm and its error model is helpful to reduce the amount of calculation and simplify the complexity of error model analysis.

Assuming that α_x and α_y are small on quasi-static base, the expansion of the error angle and velocity error equation of the damped SINS Euler platform with large azimuthal misalignment angle is obtained.

$$\begin{aligned}
&\alpha_x = -s\alpha_x\omega_N + \alpha_y\omega_U - \varepsilon_x^{n'} \\
&\alpha_y = (1-c\alpha_z)\omega_N - \alpha_x\omega_U - \varepsilon_y^{n'} \\
&\alpha_z = \alpha_x c\alpha_z\omega_N - \varepsilon_z^{n'} \\
&\delta v_x^n = (1-c\alpha_z)\widehat{f}_{sfx}^{n'} + s\alpha_z\widehat{f}_{sfy}^{n'} - (\alpha_y c\alpha_z + \alpha_x s\alpha_z)\widehat{f}_{sfz}^{n'} + c\alpha_z\nabla_{\mathrm{x}}^{n'} + s\alpha_z\nabla_y^{n'} \\
&\delta v_y^n = -s\alpha_z\widehat{f}_{sfx}^{n'} + (1-c\alpha_z)\widehat{f}_{sfy}^{n'} - (\alpha_y s\alpha_z - \alpha_x c\alpha_z)\widehat{f}_{sfz}^{n'} - s\alpha_z\nabla_{\mathrm{x}}^{n'} + c\alpha_z\nabla_y^{n'} \\
&\delta v_z^n = \alpha_y\widehat{f}_{sfx}^{n'} - \alpha_x\widehat{f}_{sfy}^{n'} + \nabla_z^{n'}
\end{aligned} \tag{12}$$

Among them $\omega_N = \omega_{ie}\cos L$, $\omega_U = \omega_{ie}\sin L$ Because the SINS algorithm with velocity damping is adopted, the right end of formula does not contain velocity error term, and the right end of Formula α_z is less than that of normal case by $-\alpha_{\mathrm{y}}s\alpha_z\omega_N$ terms, because the influence of $\mathbf{C}_{\omega}^{-1}$ is considered in this paper, the analysis is more comprehensive and accurate.

2.4 Accuracy simulation of SINS nonlinear error model

The SINS error model describes the propagation characteristics of the SINS error. The state estimation effect of the SINS error model is directly related to the accuracy of the model. In order to verify the accuracy of the nonlinear error model of SINS, the error model of GPS-aided SINS initial alignment composed of formulae is simulated. The simulation principle is shown in Fig. 1. The damping SINS algorithm and its non-damping SINS algorithm are implemented respectively under given trajectory; initial Euler platform error angle and velocity error conditions. Finally, the error between the two error algorithms is compared. The error formula is

$$\delta v_{Err}^n = \delta v^n - (\tilde{v}^n - v_g^n) \tag{13}$$

Among them, δv^n is the velocity error of the propagation calculus of the nonlinear error equation, $\tilde{v}^n$ is the velocity solution value of the damping SINS algorithm, and v_g^n is the GPS speed (i.e., the real trajectory speed).

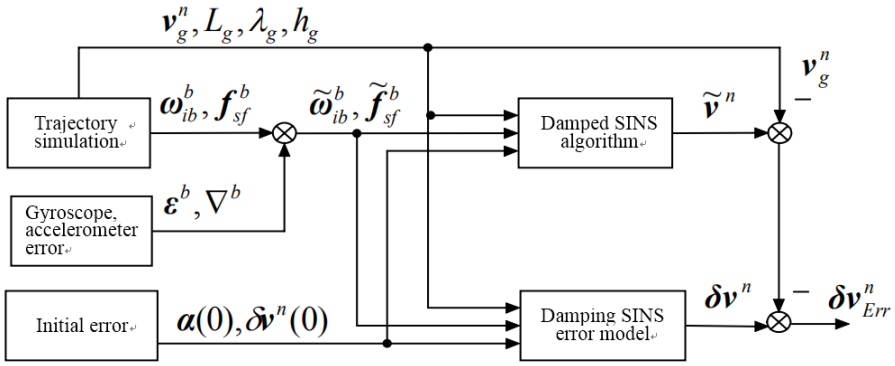

Figure 1: Simulation principle of SINS nonlinear error

The trajectory simulation design is composed of five stages.

① Given the initial value $L = 30^o$, $\lambda = 0^o$, $h = 100\,m$, $\theta = \gamma = \psi = 0^o$ drive at $10\,m/s$ north-facing and 30 s at a uniform speed;

② Acceleration 20 s to speed $30\,m/s$ with acceleration of $1\,m/s^2$;

③ Uniform speed 30 s;

④ Turn left at $9^o/s$ Jiao angle 10 s to azimuth 90^o;

⑤ A uniform speed of 30 s, a total of 120 s simulation.

3 UKF filtering based on complex additive noise

The additive noise filtering model referred to in the general literature is described below.

$$\begin{cases} x_k = f(x_{k-1}) + w_{k-1} \\ z_k = h(x_k) + v_k \end{cases} \tag{14}$$

This is referred to as simple additive noise, and the complex additive noise model referred to in this section is expressed as

$$\begin{cases} x_k = f(x_{k-1}) + g(x_{k-1})w_{k-1} \\ z_k = h(x_k) + j(x_k)v_k \end{cases} \tag{15}$$

Among them $f(\mathrm{x})$, $\mathrm{g(x)}$, $\mathrm{h(x)}$, $\mathrm{j(x)}$ and all of them can be nonlinear functions. x_k, z_k are state and measurement vectors, w_k, v_k are state and measurement noise vectors respectively. The characteristic of complex additive noise model is that the model is linear with respect to noise. Simple additive noise is a special case of complex additive noise models, but the latter is more widely used.

3.1 Standard Kalman filtering

The state equations and measurement equations of discrete linear systems can be described as follows.

$$\begin{cases} x_k = \Phi_{k|k-1} x_{k-1} + \Gamma_{k-1} w_{k-1} \\ z_k = H_k x_k + v_k \end{cases} \tag{16}$$

Formula x_k, z_k is state vector and measurement vector, $\Phi_{k|k-1}$, Γ_k and H_k are state transition matrix, noise distribution matrix and measurement matrix, w_k, v_k are system noise and measurement noise, and

$E[w_k] = 0$, $E[w_k w_j^T] = \delta_{kj} Q_k$, $E[v_k] = 0$, $E[\mathrm{v}_k v_j^T] = \delta_{kj} R_k$, $E[w_k v_j^T] = 0$, δ_{kj} is the Dirac (Dirac) function. The optimal estimation value of state x_k is obtained by measurement z_k.

3.2 Simplified UKF filtering

Standard Kalman filter is a kind of linear minimum variance estimation. The state equation is used to describe the change rule of the estimator. The state equation is driven by noise. Its state estimation algorithm is recursive. The linear algorithm framework of "prediction-correction" is adopted. UKF filtering also uses the same algorithm structure as standard Kalman filtering. The difference is that in Kalman filtering, the transfer of state statistics can be determined directly by linear equations, but not by UKF, which must evolve the transfer of state distribution characteristics by calculating sampling points.

UKF filter is based on UT transform. It carefully selects a limited number of so-called Sigma sampling points to approximate the prior statistical characteristics of the system state, and then directly evolves the posterior distribution characteristics of the system state through nonlinear equations. In UKF filtering, it is usually necessary to augment the state of system process noise and measurement noise, but when both system noise and measurement noise are additive noise; the augmentation can be avoided, which is beneficial to reduce the amount of filtering calculation. The model filtering process based on complex noise (40) is described as follows.

① Initialization of state variables and their mean square deviation.

$$\hat{x}_0 = E[x_0], \mathrm{P}_0 = E[(\hat{x}_0 - x_0)(\hat{x}_0 - x_0)^T] \tag{17}$$

② Update time

$$\begin{cases} \chi_{k-1} = [\hat{x}_{k-1}[\hat{x}_{k-1}]_L + \gamma\sqrt{P_{k-1}}[\hat{x}_{k-1}]_L - \gamma\sqrt{P_{k-1}}] \\ \chi^*_{i,k|k-1} = f(\chi_{i,k-1}) \\ \hat{x}_{k|k-1} = \sum_{i=0}^{2L} W_i^{(m)} \chi^*_{i,k|k-1} \\ P_{k|k-1} = \sum_{i=0}^{2L} W_i^{(c)} (\chi^*_{i,k|k-1} - \hat{x}_{k|k-1})(\chi^*_{i,k|k-1} - \hat{x}_{k|k-1})^T + g(\hat{x}_{k-1}) Q_{k-1} g(\hat{x}_{k-1})^T \\ \chi_{k-1} = [\hat{x}_{k|k-1}[\hat{x}_{k|k-1}]_L + \gamma\sqrt{P_{k|k-1}}[\hat{x}_{k|k-1}]_L - \gamma\sqrt{P_{k|k-1}}] \\ \eta_{i,k|k-1} = h(\chi_{i,k|k-1}) \\ \hat{z}_{k|k-1} = \sum_{i=0}^{2L} W_i^{(m)} \eta_{i,k|k-1} \end{cases} \tag{18}$$

Measurement update

$$\begin{cases} P_{\hat{z}_k \hat{z}_k} = \sum_{i=0}^{2L} W_i^{(c)} (\eta_{i,k|k-1} - \hat{z}_{k|k-1})(\eta_{i,k|k-1} - \hat{z}_{k|k-1})^T + j(\hat{x}_{k|k-1}) \mathrm{R}_k \, j(\hat{x}_{k|k-1})^T \\ P_{\hat{x}_k \hat{z}_k} = \sum_{i=0}^{2L} W_i^{(c)} (\chi_{i,k|k-1} - \hat{x}_{k|k-1})(\eta_{i,k|k-1} - \hat{z}_{k|k-1})^T \\ K_k = P_{\hat{x}_k \hat{z}_k} P^{-1}_{\hat{z}_k \hat{z}_k} \\ \hat{x}_k = \hat{x}_{k|k-1} + K_k (z_k - \hat{z}_{k|k-1}) \\ \mathrm{P}_k = P_{k|k-1} K_k P_{\hat{z}_k \hat{z}_k} K_k^T \end{cases} \tag{19}$$

Among them, $[x_k]_L$ is a matrix containing L columns, each column vector is x_k, the other parameters are calculated as follows

$$\begin{cases} \lambda = \alpha^2(\mathrm{L}+\kappa) - L \\ \gamma = \sqrt{L+\lambda} \\ W_0^{(m)} = \lambda/(L+\lambda), \quad W_0^{(c)} = \lambda/(L+\lambda) + (1-\alpha^2+\beta) \\ W_i^{(m)} = W_i^{(c)} = 1/[2(L+\lambda)], \quad (i = 1,....,2L) \end{cases} \tag{20}$$

Formula L is the dimension of state x_k, α is used to determine the distribution of a Sigma point near its mean (usually a small positive value, such as 1e_4 < α < 1), κ is a scaling factor (usually set to 0 in state estimation, $3-L$ in parameter estimation), and β is another scaling factor (used for merged state distribution). For Gaussian distribution, the optimal value is 2, and $\sqrt{\mathrm{P}}$ represents the square root matrix of matrix P (such as the lower triangular Cholesky decomposition matrix $AA^T = P$ satisfying matrix equation A).

Further, if the measurement equation in model (20) is linear, if (20) formula can be simplified to

$$\begin{cases} x_k = f(x_{k-1}) + \mathrm{g}(x_{k-1}) w_{k-1} \\ z_k = H_k x_k + v_k \end{cases} \tag{21}$$

Then we can simplify the UKF filtering algorithm, and give a brief explanation and result. In (21), the Sigma sampling point $\chi_{k|k-1}$ satisfies the equation.

$$\sum_{i=0}^{2L} W_i^{(\mathrm{c})} (\chi_{i,k|k-1} - \hat{x}_{k|k-1})(\chi_{i,k|k-1} - \hat{x}_{k|k-1})^T = P_{k|k-1} \tag{22}$$

When the measurement equation of the system is linear equation $z_k = H_k x_k + v_k$, it can get $\eta_{i,k|k-1} = H_k \chi_{i,k|k-1}$ and $\hat{z}_{k|k-1} = H_k \sum_{i=0}^{2L} W_i^{(\mathrm{m})} \chi_{i,k|k-1} = H_k \hat{x}_{k|k-1}$ from (49) formula. So there is

$$\sum_{i=0}^{2L} W_i^{(\mathrm{c})} (\eta_{i,k|k-1} - \hat{z}_{k|k-1})(\eta_{i,k|k-1} - \hat{z}_{k|k-1})^T = H_k P_{k|k-1} H_k^T \tag{23}$$

Substituting (53) formula in (49) formula $P_{\hat{z}_k \hat{z}_k}$ and taking note of $j(\mathrm{x})$ hour unit matrix is obtained.

$$P_{\hat{z}_k \hat{z}_k} = H_k P_{k|k-1} H_k^T + R_k \tag{24}$$

$$P_{\hat{x}_k \hat{z}_k} = P_{k|k-1} H_k^T \tag{25}$$

Thus, when the process noise is complex additive noise and the measurement equation is linear, the simplified UKF filtering algorithm is deduced as follows:

$$\begin{cases} \chi_{k-1} = [\hat{x}_{k-1} [\hat{x}_{k-1}]_L + \gamma \sqrt{P_{k-1}} [\hat{x}_{k-1}]_L - \gamma \sqrt{P_{k-1}}] \\ \chi^*_{i,k|k-1} = f(\chi_{i,k-1}) \\ \hat{x}_{k|k-1} = \sum_{i=0}^{2L} W_i^{(\mathrm{m})} \chi^*_{i,k|k-1} \\ P_{k|k-1} = \sum_{i=0}^{2L} W_i^{(\mathrm{c})} (\chi^*_{i,k|k-1} - \hat{x}_{k|k-1})(\chi^*_{i,k|k-1} - \hat{x}_{k|k-1})^T + g(\hat{x}_{k-1}) Q_{k-1} g(\hat{x}_{k-1})^T \\ P_{\hat{x}_k \hat{z}_k} = P_{k|k-1} H_k^T, \quad P_{\hat{z}_k \hat{z}_k} = H_k P_{k|k-1} H_k^T + R_k \\ \mathrm{K}_k = P_{\hat{x}_k \hat{z}_k} P^{-1}_{\hat{z}_k \hat{z}_k} \\ \hat{z}_{k|k-1} = H_k \hat{x}_{k|k-1}, \quad \hat{x}_k = \hat{x}_{k|k-1} + K_k (z_k - \hat{z}_{k|k-1}) \\ \mathrm{P}_k = P_{k|k-1} K_k P_{\hat{z}_k \hat{z}_k} K_k^T \end{cases} \tag{26}$$

It can be seen that the other steps of the algorithm are identical to the standard Kalman filter formula (46) except UT transformation for state and variance prediction. The simplified UKF filtering algorithm (56) avoids a series of complicated processes, such as resampling, solving multiple measurement and prediction equations, and calculating measurement and prediction errors. It is worth pointing out that the sampling strategy used in the analysis of UKF filtering simplification process is symmetrical Sigma sampling, of course, this analysis process is also applicable to simplex sampling, the latter sampling strategy can further reduce the amount of filtering calculation.

$$P_{\hat{x}_k \hat{z}_k} = P_{k|k-1} H_k^T \tag{27}$$

4 Initial alignment simulation of quasi-static base under large misalignment angle

4.1 Initial alignment filtering model

On quasi-stationary base, starting from formulas (20) and (22) and referring to the damping SINS error models (24) and (25), it is assumed that the gyro measurement error $\delta\omega_{ib}^b$ is mainly constant drift error ε^b and zero mean Gaussian white noise w_a^b. Accelerometer measurement error δf_{sf}^b is mainly constant bias error and zero mean Gaussian white noise ∇^b. Ignoring gravity error term δg^n, the state equation of the initial filtering model can be composed of the following four vector equations

$$\begin{cases} a = \mathbf{C}_{\omega}^{-1}[(I - \mathbf{C}_{n'}^{n})\omega_{in}^{n} - \mathbf{C}_{b}^{n'}\varepsilon^{b}] + \mathbf{C}_{\omega}^{-1}\mathbf{C}_{b}^{n'}w_{g}^{b} \\ \delta v^{n} = [I - (\mathbf{C}_{n}^{n'})^{T}]\mathbf{C}_{b}^{n'}\tilde{f}_{sf}^{b} + (\mathbf{C}_{n}^{n'})^{T}\mathbf{C}_{b}^{n'}\nabla^{b} + (\mathbf{C}_{n}^{n'})^{T}\mathbf{C}_{b}^{n'}w_{a}^{b} \\ \varepsilon^{b} = 0 \\ \nabla^{b} = 0 \end{cases} \tag{28}$$

It is easy to see that (28) contains the product term between the trigonometric function of the Euler platform error angle and the noise. Theoretically, these two formulas do not belong to the error model (29) of simple additive noise, but they are linear with respect to the noise term. Therefore, the UKF model proposed in the previous section must be used for filtering. Obviously, it is more difficult to obtain the Jacobian matrix of the first two loss-of-magnitude equations in (28), but this does not hinder the application of UKF filtering algorithm in initial alignment.

Suppose the state vector $x = [a^T \ (\delta v^n)^T \ (\varepsilon^b)^T \ (\nabla^b)^T]^T$, noise vector $w = [(w_g^b)^T \ (w_a^b)^T \ 0 \ 0]^T$, establish filter state model. The observational equation is established directly by taking the velocity of the damped SINS (i.e. the velocity error of the quasi-static base $z = \delta v^n$) as the observational variable.

$$\begin{cases} x = f(\mathrm{x}) + \mathrm{g}(\mathrm{x})w \\ z = Hx + v \end{cases} \tag{29}$$

Among them $H = [0 \ I \ 0 \ 0]$， v is speed measurement noise.

4.2 Initial alignment filtering model

In simulation, the initial misalignment angle α (0) selects three typical cases, which are $a(0) = [30 \ 10 \ 170]^T$, $a(0) = [0.3 \ 0.1 \ 170]^T$ and $a(0) = [0.3 \ 0.1 \ 1.7]^T$; Then three filtering methods are used to estimate the misalignment angle. They are: a) large misalignment angle UKF filtering, b) large azimuth misalignment angle UKF filtering, c) small misalignment angle standard Kalman filtering. The simulation results of alignment errors are shown in Fig. 4 to Fig. 5, in which the misalignment angle estimation errors of

real line, dotted line and dotted line are respectively those of filtering method a, b) and c, but the estimation errors of method B and C in case 1 are invalid and method C in case 2 is invalid. Out of these three curves. These typical simulation results show that the UKF filtering method based on the large misalignment error model is effective for the initial alignment estimation under various misalignment angles, and the UKF filtering based on the large azimuth misalignment error model is only suitable for the case of small horizontal misalignment angle, while the standard Kalman filtering requires three small misalignment angles.

① Generally, the estimation speed of horizontal misalignment angle is faster than that of azimuth misalignment angle. Forgotten filter algorithm is helpful to avoid the degeneration of state estimation variance matrix and gain matrix and improve the convergence speed of azimuth.

② When the misalignment angle decreases to a small value, the Kalman filter with small misalignment angle instead of UKF filter with large misalignment angle can reduce the computational complexity without losing the alignment accuracy.

③ For general nonlinear systems, it is difficult to prove the effectiveness and convergence of UKF filter theoretically, but mainly rely on Simulation and experimental verification. If the main purpose of using UKF filter under large misalignment angle is to quickly identify gross misalignment, then inertial sensors can be avoided in UKF filter model. When the difference is incorporated into the filtering model, reducing the dimension can not only reduce the amount of calculation, but also reduce the chance of divergence of UKF filtering.

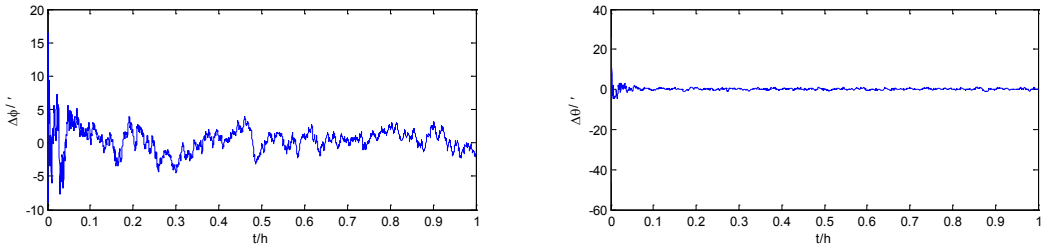

Figure 2: Alignment error of large misalignment angle

6 Conclusions

The misalignment angle between the theoretical navigation coordinate system and the calculated navigation coordinate system is expressed and the SINS nonlinear error model is derived based on the Euler platform error angle method. The simulation results under the large Euler platform error angle show that the proposed error model can accurately reflect the SINS error characteristics. Simplified UKF filtering method is deduced when both system noise and measurement noise are complex additive noise and the measurement equation is linear. The initial alignment simulation results on stationary base show that the proposed SINS error model and UKF filtering estimation algorithm are correct and effective. In order to reduce the computational complexity and ensure the stability of UKF, it is suggested that the error admission of inertial sensors is not necessary under the condition of large misalignment.

Acknowledgement: This work is funded by Natural Science Foundation of Jiangsu Province under Grant BK20160955, a project funded by the Priority Academic Program Development of Jiangsu Higher Education Institutions and Science Research Foundation of Nanjing University of Information Science and Technology under Grant20110430. Open Foundation of Jiangsu Key Laboratory of Meteorological Observation and Information Processing (KDXS1304), Open Foundation of Jiangsu Key Laboratory of Ocean Dynamic Remote Sensing and Acoustics (KHYS1405).

References

Bishop, G. (2002): Gravitational field maps and navigational errors. *IEEE Journal of Oceanic Engineering*, vol. 27, no. 3, pp. 2726-2737.

Fang, W.; Zhang, F.; Sheng, V.; Ding, Y. (2018): A method for improving CNN-based image recognition using DCGAN. *Computers, Materials & Continua*, vol. 57 no. 1, pp. 167-178.

Feng, Q.; Shen, L.; Chang, W. (2003): Gravity-aided navigation algorithm based on probabilistic data association. *Journal of Astronautics*, vol. 24, no. 5, pp. 439-443.

Fu, Z.; Wu, X.; Wang, Q.; Ren, K. (2017): Enabling central keyword-based semantic extension search over encrypted outsourced data. *IEEE Transactions on Information Forensics and Security*, vol. 12, no. 12, pp. 2986-2997.

He, Y.; Cai, T. (2006): Visual simulation system design and realization of gravity aided inertial navigation. *Chinese Journal of Scientific Instrument*, vol. 27, no. 3, pp. 2530-2531.

Huge, R.; Steven K.; Louis, M. (2004): Geophysical navigation technologies and applications. *Proceedings of the 2004 IEEE Position, Location and Navigation Symposium*. Monterey, pp. 618-624.

Li, K.; He, W.; Zhang, Z.; Zhou, Q. (2017): Node locaisation for wireless networks in smart distribution automation. *International Journal of Sensor Networks*, vol. 23, no. 1, pp. 53-60.

Liu, Z.; Liu, G. (2010): Tractor automatic navigation system based on adaptive fuzzy control. *Journal of Agricultural Machinery*, vol. 41, no. 11, pp. 148-152.

Meng, R.; Rice, S.; Wang, J.; Sun, X. (2018): A fusion stenographic algorithm based on faster R-CNN. *Computers, Materials & Continua*, vol. 55, no. 1, pp. 1-16.

Metzger, E.; Jircitano, A. (1975): Inertial navigation performance improvement using gravity gradient matching techniques. *Journal of Spacecraft and Rockets*, vol. 13, no. 6, pp. 323-333.

Qian, D.; Liu, F.; Li, Y. (2011): Comparative study on the construction method of gravity gradient reference map for navigation. *Journal of Surveying and Mapping*, vol. 40, no. 6, pp. 736-144.

Qu, F.; Li, T.; Xie, A.; Kong, Q. (2013): Application of wireless sensor networks in military. *Electronic Design Engineering*, vol. 21，no.15，pp. 34-36.

Qu, Z.; Zhu, T.; Wang, J.; Wang, X. (2018): A novel quantum steganography based on

brown states. *Computers, Materials & Continua*, vol. 56, no. 1, pp. 47-59.

Salan, S.; Eduardo, M. N.; Hugh, F. D. (1999): A high integrity IMU/GPS navigation loop for autonomous land vehicle applications. *IEEE Transactions on Robotics and Automation*, vol. 15, no. 3, pp. 572-578.

Shu, C. (2016): Research and verification of road condition optimization for floating vehicle based on WSN and GNSS fusion positioning. *Traffic Standardization*, vol. 2, no. 4, pp. 62-71.

Sun, F.; Wang, W.; Gao, W. (2009): Contour matching algorithm for passive gravity navigation. *Chinese Journal of Scientific Instrument*, vol. 30, no. 4, pp. 817-822.

Wang, J.; Zhang, X. (2011): Multi-target localization based on matched-field. *Foreign Electronic Measurement Technology*, vol. 30, no. 11, pp. 19-21.

Wei, X.; Wang, X.; Bai, X.; Bai, S.; Liu, J. (2017): Autonomous underwater vehicles lo calisation in mobile underwater networks. *International Journal of Sensor Networks*, vol. 23, no. 1, pp. 61-71.

Wu, F.; Zhang, Z. (2003): The development level and trend of passive gravity navigation technology. *Seminar on the Development Trend of Inertial Technology Development*, pp. 16-22.

Wu, H. (2010): Research on fusion localization algorithm of GNSS and wireless sensor network. *Computer Simulation*, vol. 26, no. 11, pp. 145-148.

Wu, T.; Hou, S.; Wang, K. (2009): Requirements for gravitational field aided underwater navigation for inertial navigation instruments. *Ocean Mapping*, vol. 29, no. 2, pp. 1-8.

Xiong, L.; Shi, Y. (2018): On the privacy-preserving outsourcing scheme of reversible data hiding over encrypted image data in cloud computing. *Computers, Materials & Continua*, vol. 55, no. 3, pp. 523-539.

Xu, X.; Dong, Y.; Tong, J.; Dai, W. (2017): Improved fifth-degree spherical simplex sadial cubature Kalman filter in SINS/DVL integrated navigation. *Journal of Chinese Inertial Technology*, vol. 25, no. 3, pp. 343-348.

Xu, Z.; Yan, L.; Ning, S.; Zou, H. (2007): Situation and development of marine gravity aided navigation system. *Progress in Geophysics*, vol. 22, no. 1, pp. 104-111.

Yan, J.; Xu, X.; Zhang, T.; Liu, Y.; Wu, L. (2013): Design of marine-based miniature tightly integrated SINS/GNSS navigation system. *Journal of Chinese Inertial Technology*, vol. 21, no. 6, pp. 775-780.

Zhang, T.; Chen, L.; Shi, H.; Hu, H. (2015): Underwater positioning system based on SINS/DVL and LBL interactive auxiliary for AUV. *Journal of Chinese Inertial Technology*, vol. 23, no. 6, pp. 769-774.

Zhang, T.; Xu, X.; Liu, X.; Tian, S.; Liu, Y. (2012): Time synchronization on SINS/GPS integrated navigation system under different dynamic conditions. *Journal of Chinese Inertial Technology*, vol. 20, no. 3, pp. 320-325.

Zhao, X.; Wu, J.; Zhang, Y.; Shi, Y.; Wang L. (2018): Fault diagnosis of motor in frequency domain signal by stacked de-noising auto-encoder. C*omputers, Materials & Continua*, vol. 57, no. 2, pp. 223-242.

Zhou, X.; Li, S.; Yang, J. (2008): Feature area selection in geomagnetic matching navigation. *China Inertial Technology Newspaper*, vol. 16, no. 6, pp. 694-698.